ELSEVIER

Mapping Land Surface Emissivity from NDVI: Application to European, African, and South American Areas

*Enric Valor** *and Vicente Caselles**

Thermal infrared emissivity is an important parameter both for surface characterization and for atmospheric correction methods. Mapping the emissivity from satellite data is therefore a very important question to solve. The main problem is the coupling of the temperature and emissivity effects in the thermal radiances. Several methods have been developed to obtain surface emissivity from satellite data. In this way we propose a theoretical model that relates the emissivity to the NDVI (normalized difference vegetation index) of a given surface and explains the experimental behavior observed by van de Griend and Owe. We can use it to obtain the emissivity in any thermal channel, but in this work we have focused on the 10.5- to 12.5-μm region, where most thermal sensors on board satellites work at present. The model is applicable to areas with several soil and vegetation types and where the vegetation cover changes. From the theoretical model we have developed an operational methodology to obtain the effective emissivity combining satellite images and field measurements. The error of the methodology ranges from 0.5% (due to the experimental limitations of the field methods) to 2% (considering the case in which we have no information about the studied area). To check the general validity of the model, we have validated and applied it in different atmospheric environments and in areas with a different degree of roughness, i.e., from midlatitude (France, Argentina) to tropical (Sahel, Botswana) atmospheres, and from flat (La Mancha, Spain) to rough (Valencia, Spain) surfaces, and we have obtained an error of estimate of 0.6% on the emissivity.

*Departament of Termodinàmica, Facultat de Física, Universitat de València, València, Spain

Address correspondence to Vicente Caselles, Departament de Termodinàmica, Facultat de Física, Universitat de València, 50, Doctor Moliner, 46100 Burjassot, Valencia, Spain.

Received 15 April 1995; revised 22 December 1995.

INTRODUCTION

Temperature is an important magnitude for many environmental models: (1) energy and matter exchange between atmosphere and surface, (2) weather prediction, (3) global ocean circulation, (4) climatic change, etc. We can obtain a synoptic view of this magnitude on local, regional, or global scales from thermal data provided by sensors on board satellites. These sensors directly measure the radiance emitted by the surface. Three main effects affect it: atmospheric, angular, and emissivity. This article only addresses the last aspect: the retrieval of the surface emissivity using remote sensing data.

The main problem is that it is not possible to obtain separately the temperature and the emissivity from passive radiometry, because the number of unknowns is always larger than the number of measurements (Becker, 1980). For the case of a sensor with N spectral channels, we have N equations (one per channel) for solving a problem with $N+1$ unknowns (the N emissivities plus the surface temperature). Thus the system of equations is indeterminate, and we always need some hypothesis to solve the problem.

However, some approaches that try to solve the $N+1$ unknowns problem have been recently proposed. Some are only qualitative approaches that do not permit us to know either the relative variation of the emissivity or its absolute value (Soha and Schwartz, 1978; Gillespie *et al.*, 1986). Others are quantitative methods; they permit the knowledge of the relative or absolute value of the emissivity using an additional hypothesis. Thus, for example, Watson (1992a) considered that the emissivity does not change in two different times, Kahle *et al.* (1980) assumed a constant value for the emissivity in a channel, Gillespie (1985) took the highest channel temperature as the true surface temperature, Watson

REMOTE SENS. ENVIRON. 57:167–184 (1996)

655 Avenue of the Americas, New York, NY 10010

0034-4257/96/$15.00
PII S0034-4257(96)00039-9

(1992b) related the radiance ratio to the emissivity ratio in two contiguous channels, and Coll *et al.* (1994) used radiosounding data to derive the emissivity differences between two contiguous bands.

Some methods use thermal spectral indices, such as the *TISI* (Becker and Li, 1990; Li and Becker, 1993) and the *alpha residuals* (Kealy and Hook, 1993; Hook *et al.*, 1992). Others try to relate data taken from different parts of the spectrum: *optical and microwave* domains (Becker and Choudhury, 1988), *optical and thermal* bands (Li and Becker, 1990), or *optical, thermal, and microwave* regions (Li and Becker, 1990). Some authors have studied the relationship between emissivity and some vegetation parameters or spectral indices, using radiative transfer models (Anton and Ross, 1990; Olioso, 1995) or experimental data (van de Griend and Owe, 1993).

The main inconveniences of the developed models are: (1) their complexity, because it is difficult to apply them in an operational way; (2) their error, because when the mathematical development is large the error propagation increases, and (3) their systematic errors, which can be introduced in the final result if the model approximations are not accomplished. Therefore, we propose in this article the use of an operational, mathematically simple model without systematic errors. It is based on the simple idea suggested by van de Griend and Owe (1993) and on the theoretical model developed by Caselles and Sobrino (1989). Thus, we derive the theoretical basis of the relationship between the emissivity and the NDVI proposed by van de Griend and Owe, using Caselles and Sobrino's model.

Most of the thermal sensors on board satellite systems work within the 10.5- to 12.5-μm waveband, where the emissivity values observed in the field range from 0.950 to 0.990 (Vidal, 1994). The idea of the article is to find an interpolation function between these two values, using the vegetation amount of each scene pixel. We use in this article the NDVI as a first approximation, and we consider possible improvements to the model in a possible next work.

In this article we have assumed that the vegetation and soil emissivities are known: either from field measurements or from the literature. In this sense, and as a complementary article, Rubio *et al.* (1996) have proposed two field methods and supplied a complete set of soil and vegetation emissivities.

With this objective in mind, the first part of the article presents in detail the proposed theoretical model. In the second part, we derive an operational methodology and make an error analysis with the different sources of error, to establish the capabilities and limitations of the method. In the third part, we present its validation as well as some examples of application. Finally, we discuss in the conclusions the results obtained in this study.

THEORETICAL MODEL

When observing a heterogeneous surface from a satellite, we can define the effective emissivity of the surface from the emissivities of their simple components, soil and vegetation. Therefore we need a physical model to simplify the complex surface structure. We have used the theoretical model proposed by Caselles and Sobrino (1989). It was derived following these hypotheses: (1) assuming that the ground surface is a heterogeneous—as much in temperature as in emissivity—and rough system; (2) not considering the shadows influence (thus only three elements of the heterogeneous and rough system were considered: top, ground and side); (3) neglecting double scattering processes between the different parts of the heterogeneous and rough system (top, ground, and side), which is equivalent to making an error of about 0.1°C; (4) simplifying the geometry of the heterogeneous and rough system according to the infinitely long Lambertian boxes model suggested by Sutherland and Bartholic (1977); and (5) assuming that the differences between the temperatures of the different parts of the system (top, ground, and side) are not very large (less than 30°C), (thus Planck's radiance can be expanded in Taylor series up to the first order). With these hypotheses the effective emissivity is defined as

$$\varepsilon = \varepsilon_0 + d\varepsilon, \tag{1}$$

where ε_0 represents the emissivity part corresponding to the radiation coming directly from the simple elements, and is made up by the weighted sum of their emissivities,

$$\varepsilon_0 = \varepsilon_t P_t + \varepsilon_g P_g + \varepsilon_s P_s, \tag{2}$$

where ε_t ε_g, and ε_s are the emissivities of the top, ground, and side of the roughness, respectively, and P_t, P_g, and P_s are the proportions viewed by the sensor. If we consider that the top and the side correspond to vegetation with an emissivity ε_v and a cover fraction P_v then Eq. (2) becomes

$$\varepsilon_0 = \varepsilon_v P_v + \varepsilon_g (1 - P_v). \tag{3}$$

The $d\varepsilon$ term is related to the radiation that reaches the sensor indirectly by means of internal reflections that occur between the walls and the ground of the roughness, because of the nonblackness of the natural surfaces. This effect implies that the radiation observed by the sensor is higher than the one directly emitted by the roughness elements. It is due to the so-called cavity effect of a rough surface; $d\varepsilon$ takes into account this effect and is given by (Caselles and Sobrino, 1989)

$$d\varepsilon = (1 - \varepsilon_g)\varepsilon_v F(1 - P_v) + [(1 - \varepsilon_v)\varepsilon_g G + (1 - \varepsilon_v)\varepsilon_v F']P_s, \tag{4}$$

where F, G, and F' are shape factors that take into account the fraction of radiation that reaches the ground

coming from the vegetation side, the proportion that reaches the side coming from the ground, and the fraction that reaches a side coming from the other one, respectively (see Fig. 2 of Caselles and Sobrino (1989)).

In this model we have not considered the influence of shadows because the objective of this work is only to estimate the capabilities of such a method in retrieving the emissivity. The authors treat this question in a future work, using as a starting point a more developed model that considers the influence of shadows (Caselles *et al.*, 1992).

The expression of the shape factors depends on the type of geometrical structure we use to model the roughness. If we consider the vegetation distributed by means of finite blocks we could use the shape factors corresponding to finite surfaces. But in such an approach we would be taking into account only the radiation that reaches a given surface coming from the adjacent ones, and so we would not consider the whole environment. This would lead to an underestimate of the effective emissivity. To consider all the contributions it is better to use the approximation proposed by Sutherland and Bartholic (1977), modeling the vegetation by means of infinite rows with length L, height H, and separation S (see Fig. 1 of Caselles and Sobrino (1989)). Using this configuration we substitute the radiation coming from the free spaces existing between the finite blocks by a "vegetation wall" located where each space is, and in this way we consider the infinite reflections coming from the remaining isolated boxes. Taking from Kreith (1962) the corresponding expressions of the shape factors for the energy transfer between two infinite rectangular surfaces parallel or normal, we obtain

$$F = 2\frac{H}{S}F_{s\text{-}g} = \left(1 + \frac{H}{S}\right) - \sqrt{1 + \left(\frac{H}{S}\right)^2} \tag{5}$$

$$G = \frac{S}{H}F_{g\text{-}s} = \frac{1}{2}\left\{\left(1 + \frac{S}{H}\right) - \sqrt{1 + \left(\frac{S}{H}\right)^2}\right\} \tag{6}$$

$$F' = F_{s\text{-}s} = \sqrt{1 + \left(\frac{S}{H}\right)^2} - \frac{S}{H}, \tag{7}$$

where $F_{s\text{-}g}$, $F_{g\text{-}s}$, and $F_{s\text{-}s}$ are the shape factors for the energy transference between side–ground, ground–side, and side–side, respectively, given by Kreith (1962). These last factors are not exactly the same as F, G, and F', because the first ones are applied to energy fluxes (nondirectional magnitudes) while the second ones are applied to radiances (directional magnitudes). The relationship between them is explained in Appendix A of Caselles *et al.* (1995).

We can see that $d\varepsilon$ depends on the surface structure, on the components emissivity, and on the viewing geometry [see Eq. (4)].

Once the emissivity is related to the vegetation cover of a given surface, we need a mean to obtain the soil and vegetation fractions operationally from satellite data. A simple and quick possibility is to use a vegetation index; as first approximation we have chosen the normalized difference vegetation index (NDVI) because it is very simple and widely used in remote sensing. However, possible improvements of the method using more accurate vegetation indices or techniques (SAVI, spectral mixture analysis, etc.) will be considered by the authors in a next work.

NDVI is defined as (Rouse *et al.*, 1974)

$$\mathrm{NDVI} = \frac{\rho_2 - \rho_1}{\rho_2 + \rho_1}, \tag{8}$$

where ρ_2 is the reflectance measured in the near infrared and ρ_1 is the reflectance corresponding to the red wavebands. Considering a mixed pixel with a vegetation cover P_v and a soil proportion $(1 - P_v)$, we can write, as a first approximation, that its NDVI value is

$$i = i_v P_v + i_g (1 - P_v), \tag{9}$$

where i_v and i_g are the vegetation and ground NDVI values, respectively, and i is the NDVI for the mixed surface. As i_g is usually much lower than i_v, one may think of simplifications of the previous equation. However, it is not possible in general because $(1 - P_v)$ could be higher than P_v, and in consequence the two terms of Eq. (9) could have the same order of magnitude. This equation is similar to that for the emissivity, and we can obtain the vegetation fraction from the NDVI by inverting it. But as has been pointed out by Price (1990) this relationship is not correct because the NDVI is a ratio and does not satisfy the associative property. This means that it is not the same to weigh the reflectances (which are directly measured) in each channel and then calculate the NDVI, as the inverse procedure (applied to obtain Eq. (9)). Let us see a better way to relate the NDVI to the vegetation cover. We can write a mixed pixel reflectance as

$$\rho_n = \rho_{nv} P_v + \rho_{ng} (1 - P_v), \tag{10}$$

where ρ_n is the pixel reflectance measured in the nth channel, and ρ_{nv} and ρ_{ng} are the vegetation and bare soil reflectances for the same channel. Here we have not considered internal reflections occurring inside the rough surface nor the effect of shadows. Writing this equation for the red $(n = 1)$ and near infrared $(n = 2)$ channels, and substituting into Eq. (8), the NDVI becomes

$$i = \frac{P_v(\rho_{2v} - \rho_{1v}) + (1 - P_v)(\rho_{2s} - \rho_{1s})}{P_v(\rho_{2v} + \rho_{1v}) + (1 - P_v)(\rho_{2s} + \rho_{1s})}. \tag{11}$$

Price (1990) showed that Eqs. (9) and (11) are not

equivalent. Depending on the reflectance values of each pure surface, the correction to Eq. (9) will be different.

At this point we can establish a relationship between the emissivity and the NDVI of a given surface. We rewrite Eq. (11) as

$$i = i_v P_v + i_g(1 - P_v) + di\,, \tag{12}$$

where di is a correcting factor that is calculated by subtracting Eq. (9) from Eq. (11) and that depends on the P_v value. Inverting this relationship we get P_v from the NDVI, and introducing it into Eq. (1) we finally obtain

$$\varepsilon = ai + b\,, \tag{13}$$

where

$$a = \frac{\varepsilon_v - \varepsilon_g}{i_v - i_g} \quad \text{and} \quad b = \frac{\varepsilon_g\,(i_v + di) - \varepsilon_v\,(i_g + di)}{i_v - i_g} + d\varepsilon\,.$$

For a given area the a coefficient is constant. This is not true in general for the constant b, which changes from pixel to pixel with the vegetation cover (which produces the variation of the di term) and with the surface structure (which produces the variation of the $d\varepsilon$ term). Depending on the surface characteristics, we must analyze how to handle these terms, because in specific cases they can be negligible or constant, and then Eq. (13) becomes simpler.

To see the effect of the two correcting terms ($d\varepsilon$ and di) we have simulated the variation of the effective emissivity for a heterogeneous and rough surface where the canopy density changes. We have considered the case of a vegetation with $\varepsilon_v = 0.980$, $i_v = 0.6$, $\rho_{2v} = 0.48$, and $\rho_{1v} = 0.12$, distributed on a soil with $\varepsilon_g = 0.950$, $i_g = 0.05$, $\rho_{2g} = 0.2$, and $\rho_{1g} = 0.18$. We have modeled the vegetation elements using finite boxes with dimensions $L = 0.5$ and $H = 0.4$. The S dimension varies from ∞ to 0 at the same time that the NDVI changes from i_g to i_v. Moreover we have considered vertical observation conditions, so $P_s = 0$ and $d\varepsilon$ is simplified. With these values we have generated the curves for the different corrections, corresponding in any case to a given vegetation with a defined emissivity and structure, evolving from a sparse distribution to a compact one. Figure 1 shows the results. The solid line corresponds to the linear relationship between emissivity and NDVI, $d\varepsilon$ and di being equal to 0 (combining Eqs. (3) and (9)). This case is a good approximation when these terms have negligible values, which is the case, for example, in very flat areas ($H << S$). The dotted curve describes the effect of considering only the di factor (combining Eqs. (3) and (11)); in this case the effective emissivity is lower than that in the previous one, because the use of Eq. (9) supposes an overestimation of the vegetation cover. The dotted–dashed line shows the effect of $d\varepsilon$ term (combining Eqs. (1) and (9)), which is the increase

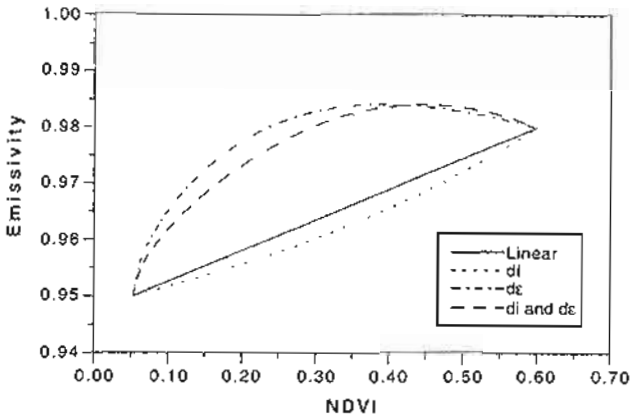

Figure 1. Effect of the different correction terms on the emissivity–NDVI relationship. (—) Linear behavior ($di = 0$, $d\varepsilon = 0$); (---) effect of introducing only the di correction ($d\varepsilon = 0$); (-·--) effect of introducing only the $d\varepsilon$ correction ($di = 0$); (– – –) total effect considering both corrections.

of the effective emissivity due to the presence of the internal reflections as we have remarked previously. Furthermore we can observe that the effects of the two correcting terms (di and $d\varepsilon$) are opposite in this simulated example. In some cases this compensation might be sufficient for validating the linear relationship, but in general terms the observed values indicate that the emissivity correction is more important than the NDVI one. Finally the dashed curve gives the general behavior represented by the complete relationship (13) (combination of Eqs. (1) and (11)); we observe a partial compensation between the two effects, which produces a slight decrease of the effective emissivity, but which is not sufficient to validate the linear relationship. Moreover the compensation is not symmetric, because of the nonsymmetry of the $d\varepsilon$ curve. This makes the general curve present an effective emissivity less than that corresponding to the $d\varepsilon$ curve until a certain NDVI value, at which point this relationship is inverted. The rapid decrease of the effective emissivity at high NDVI values is explained because the effective emissivity becomes higher than the vegetation emissivity due to the cavity effect, but at the end these two points must coincide ($\varepsilon = \varepsilon_v$).

The main conclusion we can extract from the theoretical model is that a universal relationship between emissivity and NDVI does not exist, because there are changes in the behavior linked with the emissivity values present in each area, with the structure and distribution of the vegetation and with the reflectance values measured in vegetation and in bare soil. That is, the relationship is quite dependent on the area studied. Thus, the relationship suggested by van de Griend and Owe (1993) is only applicable in areas with characteristics similar to those of the Botswana region (where the measurements were made) and cannot be extrapolated to other areas.

We can find an example of this in Owe and van de Griend (1994).

METHODOLOGY OF APPLICATION

We define the way to apply the theoretical model described above. First, we establish the error bounds of the model. The lower limit may be imposed by the field limitation in measuring the emissivity; the experimental instruments and methods and the sample heterogeneity make the observed minimum error in the emissivity measurement be 0.5% (Nerry *et al.*, 1990; Rubio *et al.*, 1996). The higher limit may be imposed by the error introduced in the temperature retrieval due to the lack of precision in the emissivity. It depends on the type of atmosphere we have in a given area, the emissivity effect being more important in the case of dry atmospheres than in the humid ones (Coll, 1994). We can consider that an error of about 1% in emissivity introduces an error of 0.6 K (0.2 K) in temperature in a dry (wet) atmosphere, if we use a single-channel algorithm, and approximately twice these values when we use a split-window algorithm. If an error of ± 1 K in the land surface retrieval can be considered acceptable at the moment, any method for the emissivity determination should not exceed an error of 1.7% (5%) in dry (wet) atmospheres using the single-channel and half of these values when using the split-window.

To define an operational methodology we have to think about the input data we need to be able to apply the developed model. Moreover we have to estimate the error depending on the available information. The application of the theoretical model has two parts. In the first one, the vegetation and bare soil proportions are obtained from the NDVI. To do that we need the reflectances in the red and near infrared channels and the NDVI values corresponding to pixels of pure vegetation and bare soil. In the second part, the effective emissivity is calculated from the proportions using Eqs. (1) to (4); in this case we need to know the vegetation and bare soil emissivities as well as the structure and distribution of the vegetation on the area. Thus, the complete information we need to apply the model exhaustively is:

- Soil emissivity, directly measured or estimated from measurements made by other authors under similar conditions of humidity and roughness.
- Vegetation emissivity (measured or estimated).
- Topographic maps of the area studied (scale 1/25000).
- Soil maps (scale 1/25000).
- Maps of natural vegetation and agricultural crops.
- Mean dimensions (H, L, S) and distribution on the area of the existing vegetation structures.
- Map of vegetation or soil fraction (if it is available, the NDVI image will be avoided).
- Reflectance images corresponding to the red and near infrared bands.
- Reflectance measurements in these bands corresponding to soil and vegetation, measured or found in the literature.
- Input data to do the atmospheric correction in the optical domain: visibility, aerosol types, type of atmosphere.

Unfortunately it is not always possible to have all the necessary data. Depending on the available information, we obtain the emissivity with an error close to 0.5% or close to 2%. The program developed for calculating emissivity maps from NDVI images was written in QuickBasic and is available upon request from the authors.

Emissivity Measurements

To calculate the effective emissivity with Eq. (1) we have to know the vegetation and soil emissivities. If we have field measurements there is no problem; but if not we can use only mean values considering the emissivity range observed experimentally. Therefore we can define an emissivity value of 0.985 ± 0.007 for vegetation considering that the experimental values usually range from 0.980 to 0.990 in the 10.5- to 12.5-μm spectral region (Schmugge, 1990; Rubio *et al.*, 1996); analogously for soils we can use a mean value of about 0.960 ± 0.010 because the experimental values observed fall between 0.950 and 0.970 in the 10.5- to 12.5-μm spectral region (Nerry *et al.*, 1990; Rubio *et al.*, 1996). This range is wider when we consider the 8- to 14-μm spectral region (See spectra given by Salisbury and D'Aria (1992)).

Vegetation Cover

We have seen two equations [(9) and (11)] for obtaining the proportions from the NDVI; they are not equivalent. Figure 2 shows this, where we have represented the curves corresponding to these two equations for the same extreme NDVI values, but for different values of the soil reflectance in the red channel. From a mathematical point of view modifications in the surface reflectances change the curve shape, making the correction additive or subtractive and higher or lower. In conclusion, it is better to use the nonlinear relationship (Eq. (11)) if it is possible. If we do not have the reflectances, we use Eq. (9).

We obtain the vegetation cover from the NDVI inverting Eq. (11),

$$P_v = \frac{(1 - i/i_g)}{(1 - i/i_g) - K(1 - i/i_v)}, \qquad (14)$$

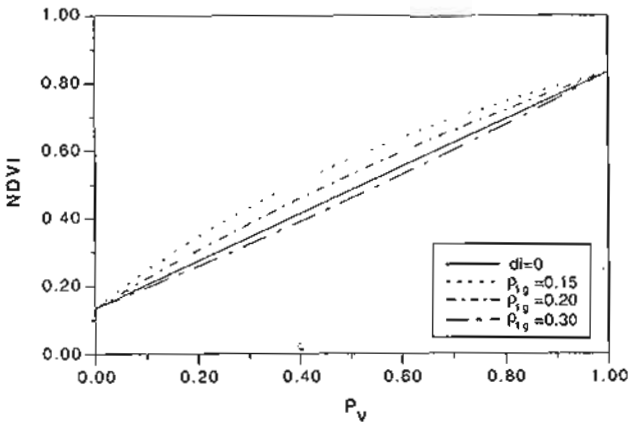

Figure 2. Effect of the *di* term for several values of the ground reflectance in the red channel (ρ_{1g}) and maintaining the extreme NDVI values unchanged. The *di* value is represented by the separation between a given curve and the solid line ($di = 0$). Depending on the reflectance values we can obtain corrections of different sign and importance.

where

$$K = \frac{\rho_{2v} - \rho_{1v}}{\rho_{2g} - \rho_{1g}} .$$

We can calculate all these factors for each image; we must determine the reflectance and NDVI values corresponding to the studied area, which can be obtained in the red and near infrared channels of the atmospherically corrected image, recognizing in it pixels with full vegetation or bare soil. Another possibility is to make field measurements of them.

Determination of $d\varepsilon$

We have seen that the error on emissivity must be less than 1–5% depending on the atmosphere type and on the correction method. So we must analyze the values that can take the $d\varepsilon$ term to see if we must always consider it or if it is negligible in some cases. To do this we consider three different approximations.

First Approximation: Flat Surface

First we consider the case of a flat surface where $H = 0$ and $P_s = 0$, the $d\varepsilon$ term being equal to zero; this is evident because in a flat surface there are no cavities in which reflections occur. The effective emissivity of such a surface will then be equal to expression (3) ($\varepsilon = \varepsilon_0$), that is, only the weighted sum of the emissivities corresponding to the different elements of the pixel. It is difficult to find surfaces strictly flat. But it is a good approximation when the H dimension is small compared to L and S. We can find such situations when the vegetation is distributed over extensive fields in a compact way (so the possible internal cavities will be taken into account when emissivity is measured in the field with the box method), the separation between the vegetated areas being larger than their mean height. In such cases the $d\varepsilon$ term is not strictly zero, but its value is small, being of the order of the minimum experimental error observed (0.5% or less).

Second Approximation: Vertical Observation

The second approximation we can consider is that corresponding to vertical observation conditions (Thematic Mapper sensor, for instance). In this case we have that $P_s = 0$ for every vegetation structure because the sensor does not observe the side of the roughness. The effective emissivity is given by Eq. (3) plus the $d\varepsilon$ term, which is simplified to

$$d\varepsilon = (1 - \varepsilon_g)\varepsilon_v F(1 - P_v) . \qquad (15)$$

We studied the values this term can take, changing the different parameters involved. We have considered different types of vegetation structures modifying the values of the geometric factors (H, L, and S). We have varied the emissivity values inside the usual range observed in the 10.5- to 12.5-μm spectral region. For the field measurements we can use radiometers working in this spectral band, but it is also possible to find instruments that operate in wider spectral ranges, such as the 8- to 14-μm region, because they are cheaper. In the 8- to 14-μm waveband, the spectral curves are usually quite "flat," and we can use in narrow bands the values measured in wider ones with a good approximation. This is true in general for vegetation; for soils and rocks we find many cases in which there is an important decrease of the emissivity in the 8- to 10-μm range due to the *reststrahlen* effect (Asrar, 1989) (absorption phenomena associated with the stretching vibrations of the Si–O bounds in the crystal lattice), and then the mean emissivity in the 8- to 14-μm region is lower than the one corresponding to the 10.5- to 12.5-μm region. In this situation we can obtain the emissivity in the narrow band from 8- to 14-μm emissivities, using linear relationships derived from spectroradiometric measurements (Rubio *et al.*, 1996).

To calculate the mean vegetation cover for a given structure we have used the finite boxes model and not the infinite rows model used in the derivation of shape factors [Eqs. (5) to (7)]. We have divided the area into equal units, each one having a vegetation box in its center surrounded by a certain soil extension. Using one of these units as reference, the vegetation cover is given by the ratio between the vegetation area and the total:

$$P_v = \frac{L^2}{(S + L)^2} . \qquad (16)$$

Following this procedure we have calculated the $d\varepsilon$ term for many cases changing the different factors. In Table 1 we show an extract of the calculations that

Table 1. Calculated Values of ε_0 and $d\varepsilon$ Terms under Vertical Observation Conditions (Eqs. (3) and (15))[a]

Type	*H (m)*	*L (m)*	*S (m)*	P_v *mean*	ε_v	ε_g	ε_0	$d\varepsilon$
Grass	0.2	2	1	0.4	0.99	0.95	0.966	0.005
						0.97	0.978	0.003
Shrub	1	1	1	0.3	0.99	0.95	0.962	0.020
						0.97	0.976	0.013
Scrub	0.5	1	0.5	0.4	0.99	0.95	0.966	0.017
						0.97	0.978	0.010
Fruit trees	3	3	2	0.4	0.99	0.95	0.966	0.021
						0.97	0.978	0.012
Pines	5	1	1	0.3	0.99	0.95	0.962	0.031
						0.97	0.976	0.019

[a] We have considered several vegetation types and used two different ground emissivities (0.950 and 0.970) to do the calculations. The vegetation cover is calculated in Eq. (16).

highlights the main result obtained. From it we can observe that

- The $d\varepsilon$ term is not negligible in general, because it can take values of 0.02 and higher. If we do not take it into account in such cases, the error in the retrieved temperature could be important (1.2 K in dry atmospheres).
- As we have commented previously, for vegetation structures that have a small mean height compared to the other two dimensions, this term can be neglected because that only supposes an error of about 0.5% or less (being of the order of the minimum experimental error we can obtain in field measurements at present).
- For a given vegetation structure the value of the $d\varepsilon$ term tends to decrease for increasing values of vegetation and soil emissivities, because the surface's reflectance decreases and consequently the cavity effect becomes less important.

Thus we cannot always neglect this term because it can suppose an excessive error in the emissivity determination. We must analyze each area studied (including its atmospheric type) and estimate if it is important or not to include the $d\varepsilon$ correction.

General Case: Oblique Observation

Finally we consider the case of oblique observation conditions, in which the effective emissivity is given by the complete Eq. (1) with all the terms involved in it. In this case the sensor sees an increasing amount of vegetation with an increasing view angle. In terms of proportions, P_t is constant because the sensor always observes the same top; otherwise P_s increases and P_g decreases and the constraint $P_t + P_p(\theta) + P_s(\theta) = 1$ is always verified.

We have studied the values that take the $d\varepsilon$ term under such conditions for two vegetation structures (shrub and pines). In each case we have put $P_t = P_v$ (mean) because under vertical observation conditions these two things are equal, and we have made P_s range from 0 to $(1 - P_t)$. Table 2 shows the results. There is a decrease in the $d\varepsilon$ term with respect to the vertical observation case. This result is meaningful because the increase of the observed vegetation proportion results in a higher value for the direct term ε_0; then $d\varepsilon$ must decrease, because the effective emissivity has a physical upper limit (the unity). Thereby, for a given vegetation structure the maximum value of the $d\varepsilon$ term is always observed under vertical observation conditions, causing a progressive decrease with increasing view angles. When we analyze the need for taking into account this term for a given area, we only have to study the vertical observation case, because it gives us the maximum possible value.

Operational Treatment of $d\varepsilon$

Now we have to deal with the question of how we can treat the $d\varepsilon$ term in an operational way, because its theoretical form is rather complicated. From Fig. 1, we can see that the shape of the curve corresponding to the general behavior of the relationship between emissivity and NDVI is quite similar to the combination of a straight line and a quadratic expression. Therefore we propose to use a quadratic form to simulate operationally the $d\varepsilon$ term. This expression takes a value of zero for $P_v = 0$ and $P_v = 1$ and a mean value $< d\varepsilon >$ for $P_v = 0.5$. Equation (1) becomes

$$\varepsilon = \varepsilon_v P_v + \varepsilon_g (1 - P_v) + 4 < d\varepsilon > P_v (1 - P_v) . \qquad (17)$$

Physically, this approximation substitutes a heterogeneous surface by another one in which there is a "mean vegetation structure" with a maximum value of $d\varepsilon$ given by $< d\varepsilon >$ and with a separation between boxes varying with P_v. Figure 3 shows the behavior of Eq. (17) for several values of $< d\varepsilon >$. We can see that increasing values of this term produce a separation from the linear behavior (when $< d\varepsilon > = 0$). Comparing these graphs with the general curve of Fig. 1, we observe that the

Table 2. Calculated ε_0 and $d\varepsilon$ Values under Oblique Observation Conditions (Eqs. (3) and (4)) for Two Vegetation Types[a]

Type	*H (m)*	*L (m)*	*S (m)*	ε_v	ε_g	P_t	P_s	ε_0	$d\varepsilon$
Shrub	1	1	1	0.99	0.97	0.3	0.0	0.976	0.012
							0.2	0.980	0.010
							0.4	0.984	0.008
							0.6	0.988	0.006
Pines	5	1	1	0.99	0.95	0.3	0.0	0.962	0.031
							0.2	0.970	0.024
							0.4	0.978	0.017
							0.6	0.986	0.010

[a] We have used P_t as a constant value, and we have changed P_s from 0 to $(1 - P_t)$ varying P_g accordingly.

operational formula (Eq. (17)) reproduces quite well the shape of Eq. (1).

To define $< d\varepsilon >$ we consider three cases as reference. First we suppose that we have no information about the vegetation structures and their spatial distribution on the area studied. This is the case of the most remote areas (Africa, South America, etc.), where vegetation maps are not available. In this case $< d\varepsilon >$ can be a mean of all the values observed for a reasonable number of distinct structures, calculated with the vegetation and soil emissivities measured, or taken from the literature, if we do not have any field measurements (see in this case, for example, the emissivity table given by Rubio *et al.* (1996)). We assume the dispersion error as the error for this value.

As an intermediate situation we can suppose that we know the types of vegetation existing in the studied site and their fractional areas. We can obtain this information from the available vegetation and soil maps. The spatial and temporal resolution of the existing maps will determine the error in $d\varepsilon$. Now we can define better the $d\varepsilon$ term calculating the values that it can take, considering only the vegetation structures existing in the zone and using mean values for their dimensions (H, L, S). Then we can calculate a weighted mean value, taking into account the proportions of each vegetation species of the area,

$$d\varepsilon_{ef} = \sum_{i=1}^{n} f_i d\varepsilon_i , \qquad (18)$$

where $d\varepsilon_{ef}$ is the weighted effective $d\varepsilon$ value, f_i is the area occupied by each species in the studied area, and $d\varepsilon_i$ is the value of the $d\varepsilon$ term for each of them. The vegetation and soil emissivities would be measured or taken from the literature. We use $d\varepsilon_{ef}$ as the mean value ($< d\varepsilon >$) to put into Eq. (17). This procedure minimizes the error because the available information permits us to concentrate on the particular vegetation structures existing in the area and then the dispersion of the values decreases.

Finally we can consider the case in which we have abundant information about the studied zone. We know all the vegetation structures, their mean dimensions, percentage, and spatial distribution, and so on. Especially useful could be a Geographic Information System (GIS) containing all the information integrated in a cartographic way. We could identify from all the maps contained in it the regions covered by each vegetation species and assign to each of them a calculated $< d\varepsilon >$ value, generating a digitalized map of $< d\varepsilon >$ terms. We would have to introduce these values into Eq. (17), changing from one area to the other with the vegetation structure. This method is applicable if we can easily recognize the areas occupied by each vegetation species; but if it is a difficult task due to a high heterogeneity or to a low resolution of the sensor, the best solution is to use a weighted mean value as has been explained (Eq. (18)).

Spatial Resolution

To apply the described model we have to identify areas of pure bare soil and areas fully vegetated. When we are working with sensors with a high spatial resolution, these areas are easy to find. But when we are using low-spatial-resolution sensors it is a more difficult task

Figure 3. Graphs corresponding to Eq. (17) for several values of $< d\varepsilon >$, where the $d\varepsilon$ term has been simulated by means of a simple quadratic form. If we compare them to the general curve of Fig. 1, we can see this expression reproduces the behavior of the $d\varepsilon$ factor quite well.

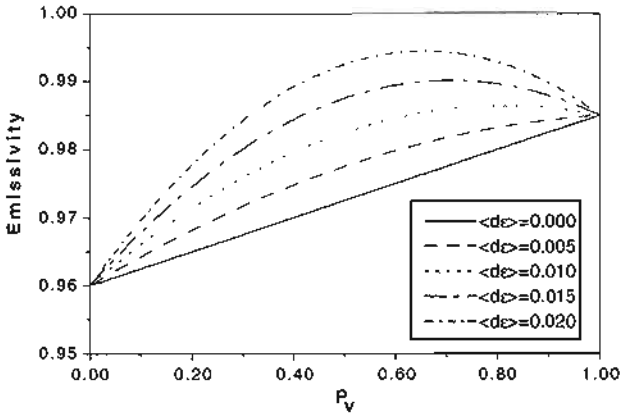

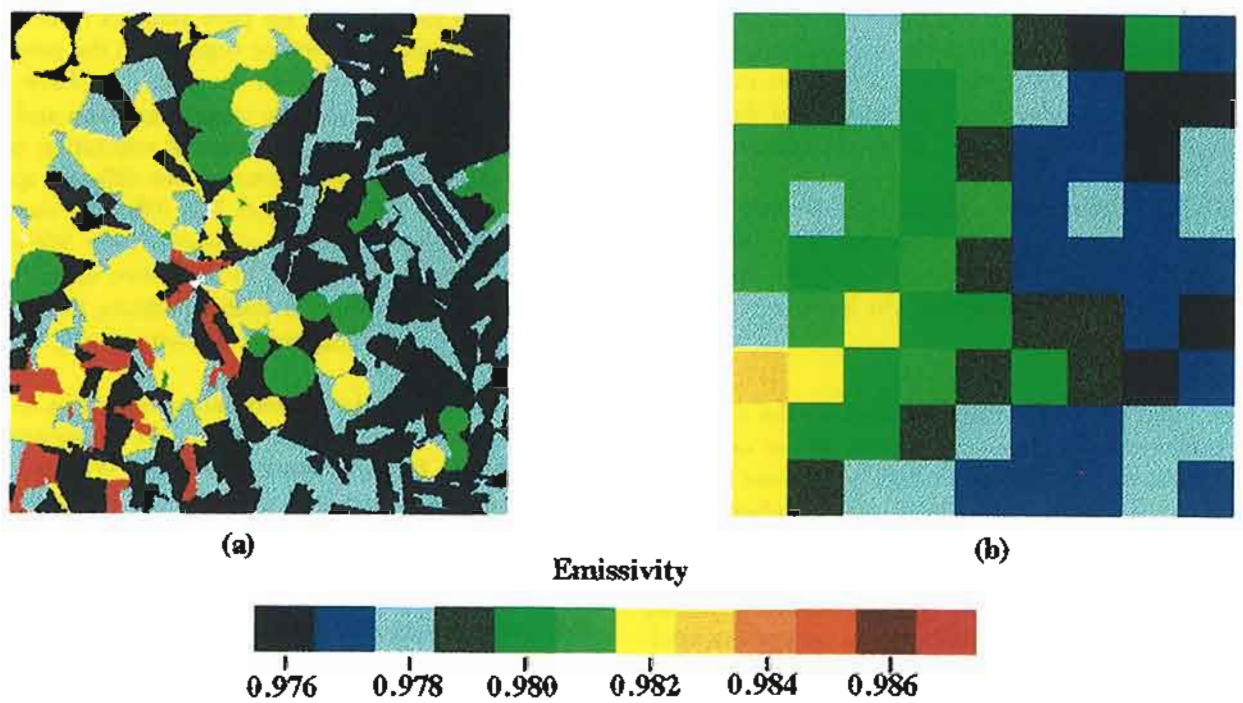

Figure 4. (a) Digitalized emissivity map of the Barrax area (Albacete, Spain) in the EFEDA Project. (b) Emissivity map degraded from a spatial resolution of 30 m to one of 1 km. The effect of the change of scale is a reduction of the emissivity range over the image. Therefore the emissivity effect will be more important in images of high spatial resolution.

because in such large pixels there is often a mixture of soil and vegetation, except if we are observing extensive homogeneous areas (such as a desert or a dense forest). In this case it is more difficult to find pure pixels, and the problems arising are how to define the NDVI values for vegetation and bare soil (that is, which values we have to assign to $P_v = 0$ and $P_v = 1$) and how we can treat the $d\varepsilon$ term.

The effect of the spatial resolution is to reduce the range of emissivity values present in a given area. This is physically evident because in large pixels we have a weighted mean value over all the surfaces existing in it. To illustrate this fact we have used a digitalized emissivity map of one of the experimental areas corresponding to the EFEDA Project: the Barrax test site, which is located near Albacete (Spain). We constructed this map using two NDVI images (dated on 12 June 1991 and 28 June 1991 respectively) obtained with data corresponding to Thematic Mapper bands 3 and 4 and several crop maps produced within the framework of this project (Barth and Runge, 1993). With this information we made a classification identifying the surfaces present in the area, and we assigned a defined emissivity value to each one, these values being measured in a field campaign. Figure 4a shows the resulting map. It has been constructed from an image with a spatial resolution of about 30 m. From it we have generated another one with an approximate spatial resolution of 1 km, dividing the image of 81 larger squares and calculating the mean value in each of them. This procedure only illustrates the physical effect of the scale change and does not simulate the response of a low-resolution sensor from data corresponding to a high-resolution one. Figure 4b shows the result of these calculations. If we compare the two images we can see that the emissivity range has been reduced to approximately half of its initial value. In fact while in the digitalized map we observe values between 0.976 and 0.987 (with a range of 0.011), in the degraded image we have values ranging from 0.976 to 0.983 (with an interval of 0.007). We can conclude that the influence of the emissivity is more important in high-spatial-resolution images than in low-resolution ones.

When analyzing images with low spatial resolution, if we use as extremes the maximum and minimum value of the image but not corresponding to pure pixels, then the emissivity range will become wider, artificially. To avoid this, we must try to select pure pixels. This is certainly not always possible, especially in areas of discontinuous vegetation such as most semiarid regions and when using larger-scale imagery such as AVHRR. One possibility is to get an area sufficiently wide for containing pure pixels of vegetation and bare soil, and use the minimum and maximum NDVI values on it. Nevertheless in semiarid areas, where this method has the greatest potential for application, it is almost impossible to find a pixel of sufficiently dense vegetation. Another possibility would be to use reflectance field

measurements of the bare soil and vegetation (under full canopy conditions) to obtain the corresponding NDVI values and retrieve the vegetation cover as explained. In this sense the existence of multitemporal datasets of field measurements covering all the conditions would be very useful.

About the treatment of the $d\varepsilon$ term the best solution in this case is to use a mean weighted value taking into account the different species existing in the area, their structures, and their proportions in it.

Error Analysis

At this point we have to discuss which are the minimum and maximum errors we can expect on the emissivity when we apply this methodology. The first one is determined by the experimental errors corresponding to field measurements, and it is about 0.5%. To calculate an estimate of the second one we have analyzed the worst situation we can find. Obviously it corresponds to having no information about the studied area except the satellite images. We do not know the emissivities nor the vegetation structures existing in it. To apply the method we use as bare soil and vegetation emissivities the proposed mean values ($\varepsilon_v = 0.985 \pm 0.007$; $\varepsilon_g = 0.960 \pm 0.010$). With them we calculate the $d\varepsilon$ terms for the vegetation structures given in Table 1, and we get as the general mean value $< d\varepsilon > = 0.015 \pm 0.008$. So Eq. (17) becomes

$$\varepsilon = 0.985P_v + 0.960(1 - P_v) + 0.06P_v(1 - P_v) . \quad (19)$$

We have applied the error theory to this equation, and we have obtained an expression for the emissivity error, which depends on the vegetation cover value,

$$\delta\varepsilon = [(\varepsilon_v - \varepsilon_g + 4 < d\varepsilon > (1 - 2P_v))^2 \delta P_v^2 + P_v^2 \delta\varepsilon_v^2 + (1 - P_v)^2 \delta\varepsilon_g^2 + 16P_v^2(1 - P_v)^2 \delta < d\varepsilon >^2]^{1/2} , \quad (20)$$

where $\delta\varepsilon$, δP_v, $\delta\varepsilon_v$, $\delta\varepsilon_g$, and $\delta < d\varepsilon >$ are the errors on the effective emissivity, vegetation cover, vegetation, soil emissivities, and on the $< d\varepsilon >$ term respectively. Table 3 shows the error on the emissivity for several values of the vegetation cover (P_v) and assuming different values for its error of estimate (δP_v). What we can expect are higher errors on P_v at low P_v values and vice versa. Consequently we can obtain the emissivity with an error of 1–2% if low vegetated pixels are observed, and this error can decrease to 0.7–1% when fully vegetated pixels are observed, the mean error being of the order of 1%.

RESULTS AND DISCUSSION

Discussion of the Model Hypothesis

In the preceding sections we have assumed that only one soil and one vegetation type exist in the area of study, but it is not true in general. Normally, we have several types of soils (sands, limestones, etc.) and different vegetations (dry, wet, healthy, etc.). The aim of this section is to validate that for pure samples (pixels with only one element: bare soil or vegetation) the proposed model is also applicable. In the field, we have both situations: (1) pixels with the same vegetation and bare soil but with different percentage of vegetation cover, and (2) pixels with only vegetation but different species and pixels with only bare soil but different moisture content, different chemical composition, etc. We check that the model is applicable in these two cases. If the model is not applicable for both situations, then it will not be applicable for mapping emissivities using satellite images.

To this end we have used data acquired by us in a field campaign carried out within the framework of the DEMON Project during July 1994. We made the measurements in two experimental sites located in the Hérault and the Ardèche regions (southern France). These sites are representative of Mediterranean areas on limestone substrate; crystalline substrate would probably present different features, especially concerning soil emissivity. The main vegetation structures we can find correspond to a typical Mediterranean environment, representing deciduous and evergreen oak forests and various types of degraded woodlands and rangelands. In addition to this natural vegetation we can find several types of crops, chiefly vineyard, wheat, barley, almond trees, and mulberry trees. We made emissivity measurements of several soil and vegetation types using a field thermal radiometer working in the 8- to 14-μm interval and by means of the box method developed by the University of Valencia (Caselles *et al.*, 1995). Reflectance measurements were made at the same time with a radiometer, which simulates the bands of the SPOT-XS sensor, from which NDVI values were derived. Dr. B. Lacaze (CNRS / CEFE, Montpellier) processed and supplied these last measurements. Table 4 shows the surface types and their measured emissivity and NDVI values.

From these data we have calculated the mean value of the emissivities and reflectances corresponding to the different soils present in the area to define a "unique value" to use in the model. We have obtained $\varepsilon_g = 0.951 \pm 0.009$, $\rho_{1g} = 0.24 \pm 0.08$, $\rho_{2g} = 0.30 \pm 0.09$, $NDVI_g = 0.1 \pm 0.2$. Similarly for the vegetation (using only the samples with higher emissivity and NDVI) we have obtained $\varepsilon_v = 0.986 \pm 0.007$, $\rho_{1v} = 0.065 \pm 0.013$, $\rho_{2v} = 0.4 \pm 0.1$, $NDVI_v = 0.72 \pm 0.08$. Using for the geometrical dimensions the values $L = 5$ m, $H = 1$ m we obtain a theoretical curve that fits the experimental points with an error of estimate of 0.6% in emissivity (see Fig. 5), which confirms the validity of the model in the case of the existence of different soil and vegetation samples in a given area.

Model Validation

We made a complete model validation using the data published by van de Griend and Owe (1993), obtained

Table 3. Error on the Effective Emissivity for the Worst Case of Application (Eq. (20)), Considering Several Values of the Vegetation Cover (P_v) and of Its Error (δP_v)

	δP_v			
P_v	0.05	0.10	0.15	0.20
0.00	0.011	0.013	0.016	0.020
0.25	0.010	0.011	0.013	0.015
0.50	0.010	0.010	0.011	0.011
0.75	0.008	0.008	0.008	0.008
1.00	0.007	0.008	0.009	0.010

within the framework of the project *Botswana Water and Surface Energy Balance Research Program*. These data consider both cases: different types of vegetation and different vegetation cover. The studied area consists mainly of savannah vegetation and agricultural crops. The authors made emissivity measurements for several types of surfaces in the 8- to 14-μm spectral region using the box method developed by the University of Strasbourg (Becker *et al.*, 1986). Reflectance measurements were simultaneously made for the same surfaces using a radiometer designed at the Goddard Space Flight Center (NASA), which simulates the red–green and near infrared bands (1 and 2) of the AVHRR sensor. The measurements were made on 10 different surfaces. Van de Griend and Owe (1993) obtained an experimental relationship given by

Table 4. Reflectance, NDVI, and Emissivity Values, along with Their Respective Standard Deviations, of Several Surfaces Corresponding to the Hérault and Ardèche Areas (Southern France) and Measured in a Field Campaign in the Framework of the DEMON Project, July 1994

Samples	$\rho_2 \pm \sigma_{\rho 2}$	$\rho_3 \pm \sigma_{\rho 3}$	$NDVI \pm \sigma_{NDVI}$	$\varepsilon \pm \sigma_\varepsilon$
Bare soil Hérault	0.338 ± 0.005	0.396 ± 0.003	0.079 ± 0.008	0.947 ± 0.005
Bare rock (white limestone)	0.363 ± 0.004	0.444 ± 0.012	0.100 ± 0.014	0.948 ± 0.008
Bare rock (gray limestone)	0.144 ± 0.011	0.220 ± 0.011	0.21 ± 0.04	0.951 ± 0.004
Marl	0.237 ± 0.010	0.251 ± 0.015	0.03 ± 0.04	0.955 ± 0.008
Bare soil (clay in vineyard)	0.280 ± 0.019	0.340 ± 0.017	0.10 ± 0.04	0.952 ± 0.009
Bare soil (brown, uprooted vineyard)	0.23 ± 0.03	0.29 ± 0.02	0.12 ± 0.07	0.951 ± 0.019
Bare soil (vineyard)	0.222 ± 0.004	0.283 ± 0.004	0.121 ± 0.011	0.954 ± 0.006
Bare soil (brown, melon field)	0.134 ± 0.003	0.189 ± 0.004	0.170 ± 0.015	0.948 ± 0.012
Shrub: rosemary (*Rosmarinus officinalis*)	0.0700 ± 0.0005	0.2300 ± 0.0018	0.533 ± 0.004	0.975 ± 0.007
Shrub: box (*Buxus sempervirens*)	0.0420 ± 0.0010	0.254 ± 0.003	0.716 ± 0.006	0.991 ± 0.006
Shrub: juniper (*Juniperus oxycedrus*)	0.090 ± 0.002	0.2390 ± 0.0013	0.453 ± 0.009	0.981 ± 0.006
Herbaceous species (*Brachypodium retusum*)	0.129 ± 0.013	0.285 ± 0.014	0.38 ± 0.05	0.976 ± 0.009
Tree: downy oak (*Quercus pubescens*)	0.067 ± 0.009	0.53 ± 0.05	0.78 ± 0.03	0.983 ± 0.008
Tree: pine (*Pinus nigra*)	0.060 ± 0.009	0.45 ± 0.02	0.76 ± 0.03	0.982 ± 0.009
Herbaceous species (*Aphyllantes monspeliensis*)	0.081 ± 0.010	0.256 ± 0.014	0.52 ± 0.05	0.990 ± 0.004
Alfalfa (*Medicago sativa*)	0.074 ± 0.001	0.539 ± 0.011	0.759 ± 0.005	0.987 ± 0.004
Vineyard (*Vitis vinifera*)	0.0810 ± 0.0008	0.47 ± 0.02	0.706 ± 0.011	0.985 ± 0.003
Straw (partial cover)	0.193 ± 0.005	0.337 ± 0.005	0.272 ± 0.014	0.975 ± 0.011
Straw (total cover)	0.12 ± 0.02	0.298 ± 0.016	0.43 ± 0.07	0.977 ± 0.003
Herbaceous species (*Brachypodium pinnatum*)	0.1390 ± 0.0019	0.412 ± 0.015	0.495 ± 0.015	0.990 ± 0.005
Tree: holm oak (*Quercus ilex*)	0.063 ± 0.006	0.38 ± 0.03	0.70 ± 0.03	0.985 ± 0.010

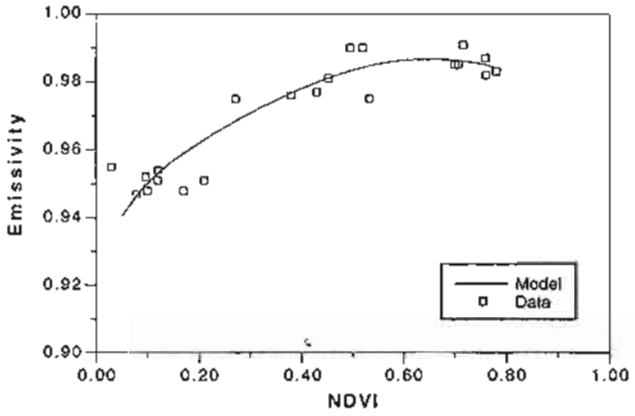

Figure 5. Validation of the capability of the theoretical model in reproducing the variation of the emissivity with the NDVI in the case of pure pixels. Data measured in the Hérault and Ardèche regions (Southern France) have been used in this validation. Using $L = 5$ m and $H = 1$ m we obtain a relationship that fits the experimental points with an estimate error of 0.6% in the emissivity.

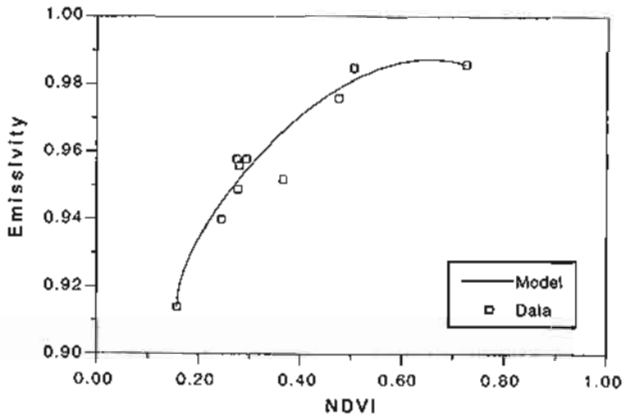

Figure 6. Complete validation (both sample change and cover change) of the theoretical model, using data measured by van de Griend and Owe (1993) in the Botswana region. With $L = 0.6$ m and $H = 0.6$ m we obtain a theoretical relationship that fits the experimental points with an estimate error of 0.6% in the emissivity.

$$\varepsilon = 1.0094 + 0.047 \ln(\mathrm{NDVI}), \qquad (21)$$

with an estimate error of 0.7% in the emissivity.

We have used these data to check our model. We have chosen as extreme emissivities the one corresponding to bare soil (0.914) and that for vegetation (0.986) and their NDVI values (0.157 and 0.727 respectively). The low value corresponding to the bare soil emissivity may be due to the existence of *reststrahlen* bands within the 8- to 14-μm band used in the measurements. We have used for the reflectances in the red and near infrared bands of soil and vegetation the values given by van de Griend and Owe (1993). Using these data we have followed the procedure explained in the theoretical model (Eq. (13)), and we have considered vertical observation conditions. We have observed that if we vary the geometric dimensions (L, H) the different curves fit groups of experimental points. This may be because we have different vegetation structures in the data, where a unique line fitting all of them perfectly does not exist. Nevertheless choosing appropriate mean values for L (0.6 m) and H (0.6 m) we can find a relationship that fits quite well to the experimental data (see Fig. 6), with an error of estimate of 0.6% in emissivity. Then we can conclude that the developed model can be applicable for the emissivity mapping, provided that it accounts quite well both for the vegetation cover change and for the sample change in a given area.

Applications

We have applied the described operational methodology to four different regions, covering several atmospheric conditions and degrees of roughness, and with different levels of information. In each case we have analyzed the maximum error we can expect in the emissivity determination, in terms of the available data and their corresponding errors.

Application to the Sahelian Area

The first example corresponds to the experimental area of the HAPEX-Sahel (*Hydrologic Atmospheric Pilot Experiment in the Sahel*) Project. It has an extension of 100×100 km^2 and is located in the Sahel (Niger) transitional zone between the desert in the north and the vegetated region in the south. In this case the available information is the measured emissivity of the desert sand, the satellite images (NOAA/AVHRR), and some knowledge of the type of structures present in the area. The emissivity measurements were carried out by the University of Strasbourg using a spectroradiometer. A value of $\varepsilon_g = 0.960 \pm 0.005$ was obtained in the 10.5- to 12.5-μm spectral region for this surface (Stoll and Pion, 1993). Since we do not have emissivity measurements for the vegetation, we have used the proposed mean value $\varepsilon_v = 0.985 \pm 0.007$.

To estimate the value of $< d\varepsilon >$ we have considered the main surfaces existing in the area. There are three types of vegetation mainly: fallow-savannah, tiger-bush, and millet; we have calculated the values of the $d\varepsilon$ term for each one of these surfaces, taking into account their dimensions and that we are working at the scale of AVHRR. Table 5 gives the results. The fallow-savannah consists of shrubs sparsely distributed on a soil covered by annual herbs, so we take $\varepsilon_g = 0.985$ because the soil is covered by vegetation. In this case the top, side, and ground of roughness are constituted by the same type of surface. We have considered that the fallow-savannah is sufficiently extended to cover more than one AVHRR pixel, so we have modeled the roughness substituting each shrub by a box; using the available information on

Table 5. Values of the $d\varepsilon$ Term Calculated for the Main Surfaces Present in the Sahelian Area[a]

Surface	*Proportion (%)*	ε_g	ε_v	H (m)	L (m)	S (m)	$d\varepsilon_{max}$
Bare soil	25	0.960					
Fallow-savannah	25	0.985	0.985	2.5	3.5	5	0.005
Tiger-bush	25	0.960	0.985	6	20	50	0.003
Millet	25	0.960	0.985	2.5	0.5	1.1	0.03

[a] We have used the mean dimensions found in the bibliography (Coutorbe *et al.*, 1992; Coutorbe, 1993), and the ground emissivity measured *in situ*. Equal fractional areas for the several vegetation types have been assumed. With these values we have obtained $< d\varepsilon > = 0.011 \pm 0.010$.

the vegetation characteristics (Coutorbe *et al.*, 1992; Coutorbe, 1993) we have considered as mean dimensions $L = 3.5$ m, $S = 5$ m, and $H = 2.5$ m. With these values we have calculated $d\varepsilon$ in the case of vertical observation conditions (Eq. (15)) and we have obtained $d\varepsilon = 0.005$. The tiger-bush consists of dense strips of woodland (with trees 4–8 m high) separated by wider strips of completely bare soil. The strips of vegetation are 10–30 m wide, 100–300 m long, and separated by 50 m approximately. This fact allows there to be several strips in a given pixel, so the best way to model the roughness is to consider infinitely long boxes (substituting the vegetation strips) with dimensions $L = 20$ m, $S = 50$ m, and $H = 6$ m. In this case the calculations give us $d\varepsilon = 0.003$. The millet is the principal crop of the area. The plants are sown at intervals of 0.75 m in rows 1.5 m apart and have a mean height of 2.5 m. Modeling the surface taking each plant as a box and using $L = 0.5$ m, $S = 1.1$ m, and $H = 2.5$ m we obtain $d\varepsilon = 0.03$. Since we did not have information about the fractions of each type of vegetation and bare soil in the whole area, we calculated $< d\varepsilon >$ considering the same proportion of each of these four surfaces, thus obtaining $< d\varepsilon > = 0.011 \pm 0.010$.

The reflectance and NDVI images were processed and corrected geometrically and atmospherically (Kerr *et al.*, 1993). We applied previously a procedure for eliminating the clouds (Saunders and Kriebel, 1988). Then we looked for the extreme NDVI values of the image, and we took the minimum and maximum values, checking that they did not correspond to cloudy or watery pixels, and the corresponding reflectance values in the red and near-infrared channels. Figure 7 shows the difference between Eqs. (9) and (11), from which we see that in this case the correction (di) is very small. In terms of vegetation cover it supposes an error less than 5%. Finally, following the procedure explained in Eqs. (14) and (17), we obtained the emissivity image (see Fig. 8); we can see an increase of the emissivity value in the north–south direction, following the transition between the desert and the vegetated area. The error analysis gives for this situation a maximum error in the determination of the emissivity of 1.5%.

Application to the Mendoza Oasis

The second example corresponds to the Mendoza oasis (Argentina), studied in the framework of the project *Hydrological Determinants of Agriculture in South America: Remote Sensing and Numerical Simulations*. It is a highly cultivated area that is irrigated artificially with the water of the Tunuyan river and is surrounded by a desert (less than 200 mm of rainfall per year). The available information is the satellite images (Landsat / Thematic Mapper), vegetation maps, and the dimensions of the vegetation types. We have no emissivity measurements, thus we have used the proposed mean values.

We have calculated $< d\varepsilon >$ considering the vegetation types of the area. We can find two types of vineyard: one is planted in rows with mean dimensions $L = 0.6$ m, $S = 2$ m, and $H = 1.3$ m; in this case we have calculated the mean P_v considering the infinite rows approximation, and we have obtained $d\varepsilon = 0.014$. The other type is constituted by vine arbors, which cover completely the soil, thus $d\varepsilon = 0$. There are also fruit trees with $L = 2$ m, $S = 2$ m, and $H = 3$ m; here we have considered finite boxes for modeling the trees, and we

Figure 7. Graphs of the di factor (difference between Eqs. (11) and (9)) for the Sahel, Mendoza, Valencia, and La Mancha experimental areas. With these examples we can clearly see that the correction can be large or small, and of different sign, depending on the particular reflectances measured in a given area. Thus we must always apply Eq. (11) if it is possible.

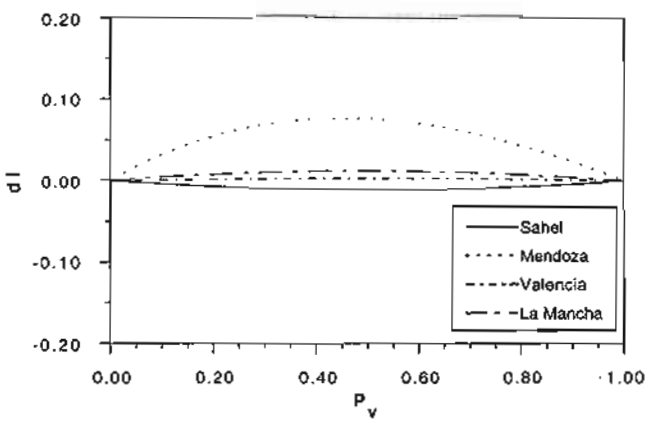

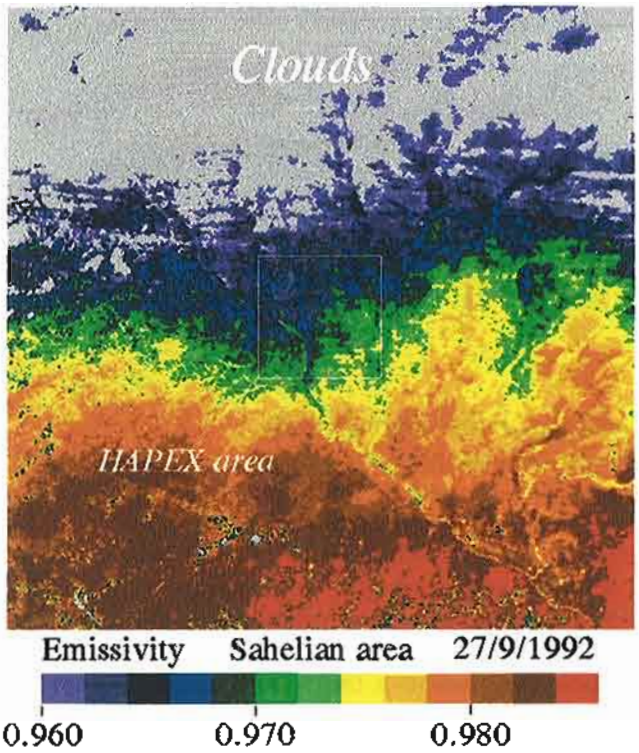

Figure 8. Emissivity map of the Sahelian area at NOAA / AVHRR scale. Previous to the calculations a procedure for removing the clouds (marked in gray) has been applied (Saunders and Kriebel, 1988). We can see an increasing emissivity from North to South, following the transition from the desert to the vegetated area. It is possible to follow the course of the Niger river in the lower half of the image flowing in the NW–SE direction. The pilot site of the HAPEX Project is marked with a white square.

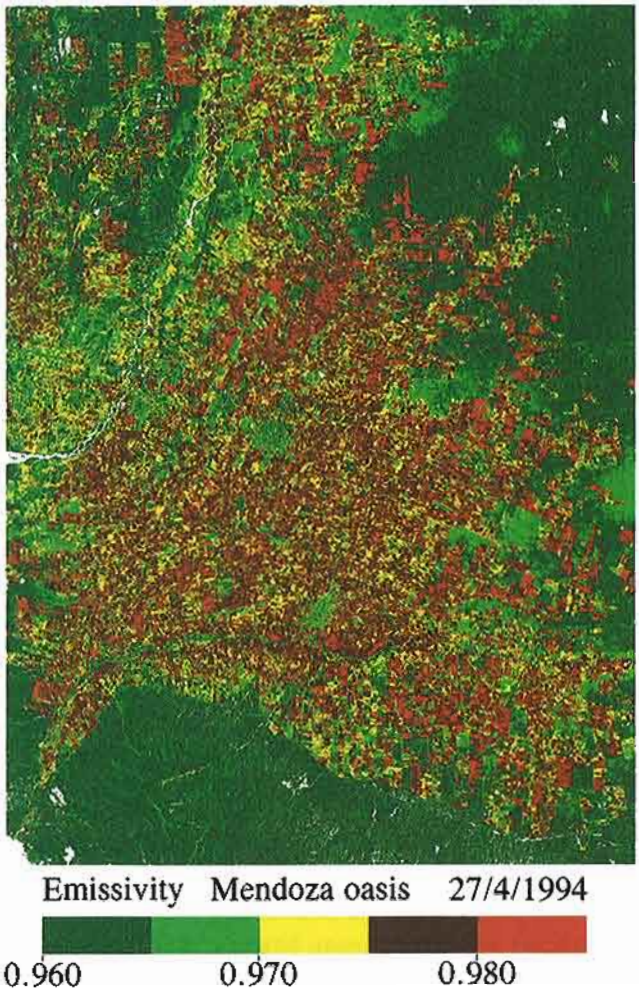

Figure 9. Emissivity map of the Mendoza oasis at Landsat / Thematic Mapper scale. White pixels mark watery surfaces. We can clearly see the contrast between the oasis (in the center, higher emissivities) and the desert (in the surroundings, lower emissivities). In the oasis we can observe the fields well defined and the high density of the crops, which makes the emissivity high in this area.

have obtained $d\varepsilon = 0.020$. We have treated similarly the olive trees, which have dimensions $L = 4$ m, $S = 6$ m, and $H = 5$ m, and we have obtained $d\varepsilon = 0.018$. Table 6 shows these values together with the fractions estimated using a vegetation map. With Eq. (18) we have obtained $< d\varepsilon > = 0.004 \pm 0.007$.

We have calculated the reflectances in channels 3 and 4 and the NDVI. Figure 7 shows the *di* term for this case, which is important (a maximum error of 10% in terms of vegetation cover). Combining Eqs. (14) and (17) with the appropriate coefficients, we have calculated the emissivity image, shown in Fig. 9. We can see clearly the contrast between the desert and the vegetated areas. The error analysis gives a maximum expected error of 1.4%.

Application to the Valencian Area

The third example corresponds to the experimental area of the DEMON (*An Integrated Approach to Mediterranean Land Degradation Mapping and Monitoring by Remote Sensing*) Project located in Buñol, near Valencia (Spain). It is a very heterogeneous zone, in which the main natural vegetation is shrub and coniferous, and the principal crops are vineyards and fruit trees. The available information is the bare soil and vegetation emissivities, the satellite images (Landsat / Thematic Mapper), and topographical maps of the area (scale 1 / 25000). In a field campaign carried out in March–April 1993 we measured the emissivity of several surfaces in the area. We obtained a value of 0.958 ± 0.005 for bare soil emissivity and of 0.986 ± 0.005 for vegetation emissivity (Rubio *et al.*, 1996).

We have modeled all the vegetation types substituting each vegetation element (tree, shrub, etc.) by a box. Table 7 shows the main vegetation types, their fractional areas in the zone (estimated from the topographical maps), and the mean dimensions. From these data we have calculated the values of the $d\varepsilon$ term following the same procedure as for the previous cases. To calculate

Table 6. Values of the $d\varepsilon$ Term calculated for the Main Surfaces Present in the Mendoza Oasis[a]

Surface	*Proportion (%)*	ε_g	ε_v	*H (m)*	*L (m)*	*S (m)*	$d\varepsilon_{max}$
Bare soil	59.5	0.960					
Vine arbours	15.0	0.960	0.985	2		3	0.000
Vineyards in rows	8.5	0.960	0.985	1.3	0.6	2	0.014
Fruit trees	8.5	0.960	0.985	3	2	2	0.020
Olive trees	8.5	0.960	0.985	5	4	6	0.018

[a] We have no emissivity measurements. The mean dimensions and fractional areas for the vegetation types have been obtained from vegetation maps. With these values we have obtained $<d\varepsilon> = 0.004 \pm 0.007$.

$<d\varepsilon>$ we have used Eq. (18), weighting the $d\varepsilon$ values of the several surfaces with their fractions in the area; we have obtained $<d\varepsilon> = 0.010 \pm 0.006$.

We have calculated channels 3 and 4 reflectances and the NDVI. Figure 7 shows the *di* correction, equivalent to an error less than 3% in vegetation cover. With these three examples we can observe that the *di* term can have a different behavior, being positive (Mendoza, Valencia) or negative (Sahel), and with a low (Sahel, Valencia) or high (Mendoza) value, depending on the particular reflectances presented by the vegetation and the soil. Figure 10 shows the emissivity image obtained applying the described methodology. Now the error analysis gives a maximum expected error of 1.4%.

Application to La Mancha Area

The last example corresponds to one of the experimental areas of the EFEDA (*Echival Field Experiment in a Desertification-Threatened Area*) Project. It is a 10×10 km^2 area located in Barrax near Albacete (Spain). In it there is bare soil mixed with crop fields of barley, corn,

Figure 10. Emissivity map of the Valencian area at Landsat / Thematic Mapper scale. Gray pixels mark urban areas, roads and a reservoir. The central part of the image (blue–green colored) corresponds to a degraded area, in which we can find mainly brushwood sparsely distributed and small fields of fruit trees and vineyards. The lower and left areas correspond to pine forests that have been affected by wildfires the last years. It is possible to follow the course of the Xuquer river (red pixels at the middle part of the image). The red areas in the upper right corner of the image correspond to fields of orange trees.

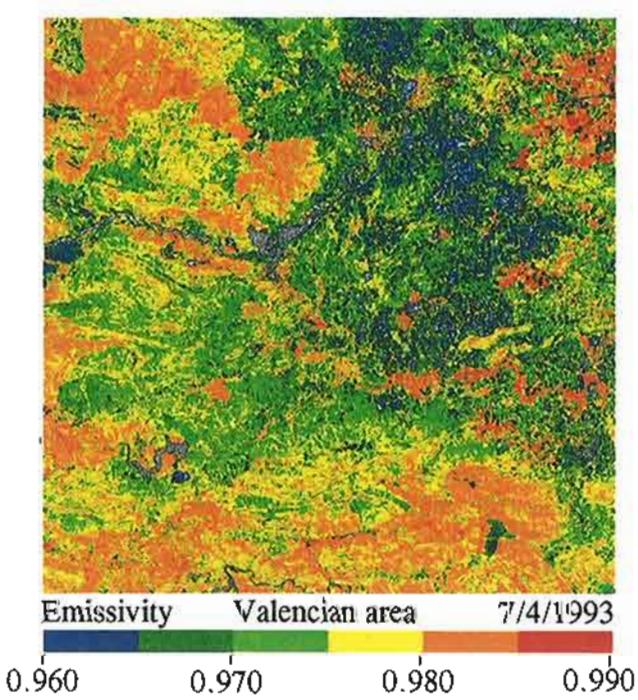

Figure 11. Emissivity map of La Mancha area at Landsat / Thematic Mapper scale. Blue pixels correspond to areas of bare soil; green pixels are areas of dry barley and fields of maize and wheat; areas in yellow–orange are primarily fields of irrigated barley; and pixels in red correspond to alfalfa. Each circle is a "pivot" which consists of an irrigation system that moves in circles around a center and irrigates the field while moving.

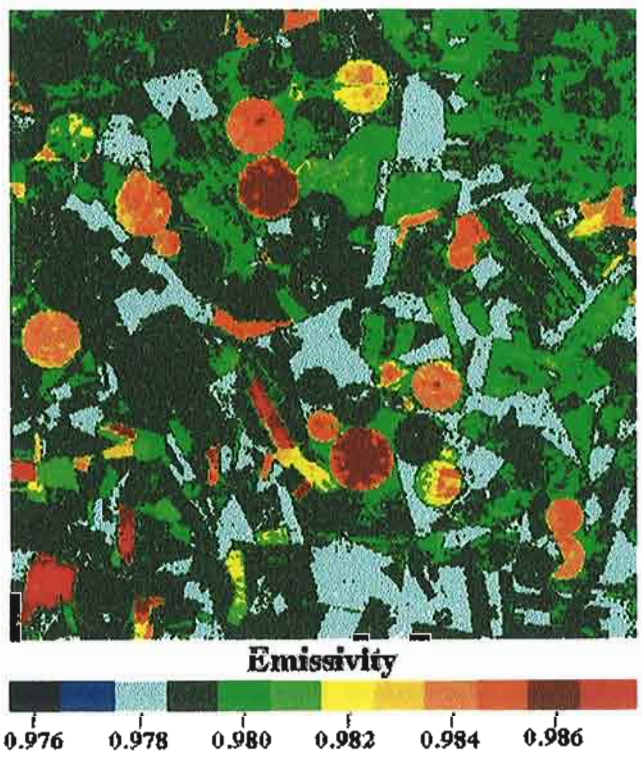

Table 7. Values of the $d\varepsilon$ Term calculated for the Main Surfaces Present in the Valencian Area[a]

Surface	*Proportion (%)*	ε_g	ε_v	H *(m)*	L *(m)*	S *(m)*	$d\varepsilon_{max}$
Bare soil	34	0.958					
Scrub	28	0.958	0.986	1	1	1	0.017
Coniferous	9	0.986	0.986	5	1	1	0.009
Vineyard	15	0.958	0.986	2	0.25	6.6	0.011
Fruit trees	14	0.958	0.986	3	3	2	0.017

[a] We have used the ground and vegetation emissivities measured *in situ* and the mean dimensions found in the field. The fractional areas for the several vegetation types have been estimated using the available topographic maps. With these values we have obtained $\langle d\varepsilon \rangle = 0.010 \pm 0.006$.

wheat, alfalfa, and vegetables mainly. In this case we have information on the emissivities of the several surfaces present in the area, the satellite images (Landsat / Thematic Mapper), and detailed topographical and crop maps. In a field campaign carried out in 1991 we measured the emissivity of the different surfaces, obtaining a value of 0.978 ± 0.005 for bare soil and 0.987 ± 0.007 for vegetation.

Regarding the $d\varepsilon$ term, we analyzed the structure of the zone. It is a quite flat area where cultivated fields alternate with extensive bare soils. The different crop types show a dense structure. The internal reflection effect is small inside a given crop (due to its compactness) and it is also small between cultivated fields because their separation is large compared to their mean heights. Then the "flat surface" approximation may work in this situation. Consequently we have used a value of 0 for the $d\varepsilon$ term.

From the reflectance and NDVI values of soil and vegetation we have calculated di (see Fig. 7), being positive and small (equivalent to an error less than 5% in vegetation cover). Thus, this case would be a good example of a simple linear relationship to map the emissivity. Figure 11 shows the result. In this third situation the error analysis gives a value of 0.7%.

We have made a new validation comparing this image to the digitalized one given in Fig. 4a, performing the difference between them on a pixel by pixel basis. Figure 12 shows the image of the difference. Values of 0 were obtained over bare soil areas and alfalfa fields; this result was expected, because the extreme emissivity values corresponded to these two surfaces. We observed differences between 0 and 0.002 on maize fields and values ranging from 0.004 to 0.006 corresponding to some fields of alfalfa that were not cultivated at the time the image was taken. Differences ranging from 0 to -0.004 were obtained on dry and some irrigated barley fields, and finally the highest differences, ranging from -0.004 to -0.006, were observed over irrigated barley fields. Moreover we have obtained a mean value of the differences of -0.0008 with a standard deviation of 0.003. This result is quite good and encourages a deeper study and development of the model and the operational method.

CONCLUSIONS

In this work we have developed a theoretical model that relates the emissivity to the NDVI and is capable of explaining the experimental behavior observed by van de Griend and Owe (1993). The effective emissivity is broken direct (ε_0) and reflection ($d\varepsilon$) terms, which are functions of the soil and vegetation emissivities, of the proportions observed by a sensor, and of its particular structure (H, L, S). The vegetation cover is obtained from the NDVI. Thus this vegetation parameter, common element of the effective emissivity and NDVI, is the connection that permits us to link these two magnitudes in a certain relationship. From this theoretical model we have developed an operational methodology to obtain the effective emissivity of a given area from satellite images. We have analyzed the possible approximations and the ways to treat the main questions that can arise in the proposed procedure. We have seen that the lack of precision in the emissivity can produce large errors in the temperature determination. Thus we cannot always neglect the $d\varepsilon$ term. We have to analyze each area studied in terms of its structure and the particular atmospheric conditions.

An analysis of the error bounds in the application of this methodology has led us to the conclusion that the minimum error we can achieve in the emissivity determination is 0.5% mainly due to the experimental limitations of the current field methods. The maximum error we can expect is about 2% considering the case in which we have no information about the area of study except the satellite images. We have made two validations using field data to check the applicability of the theoretical model in two very different environments. In these two cases we have seen that the model fits the data with an error of estimate of 0.6% in emissivity.

Finally, we have presented several images produced by application of the exposed methodology. Moreover

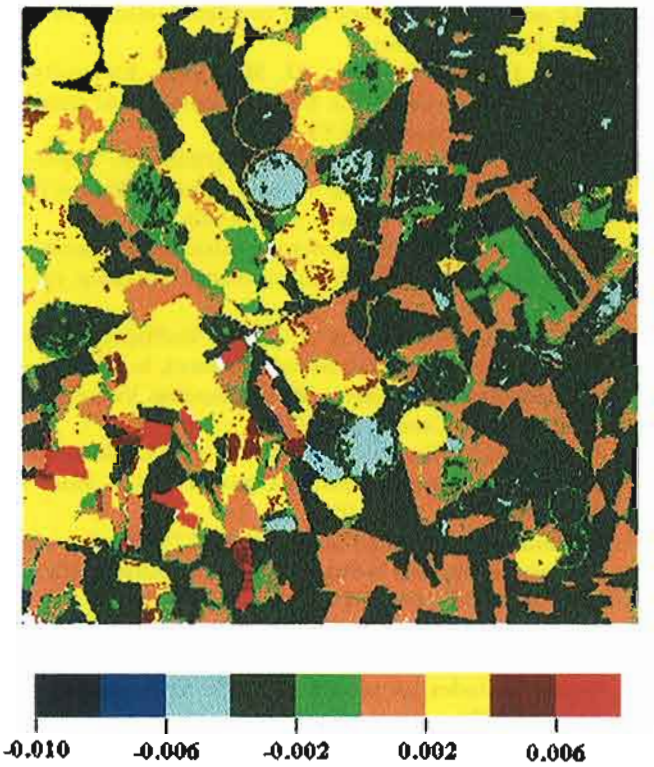

Figure 12. Difference between the calculated and digitalized maps for the Barrax area. $\delta\varepsilon = 0$; bare soil areas and alfalfa fields; $\delta\varepsilon = 0$ to 0.002; maize fields; $\delta\varepsilon = 0.004$ to 0.006: some fields of alfalfa that were not cultivated at the time the image was taken; $\delta\varepsilon = 0$ to -0.004: dry and some irrigated barley fields; $\delta\varepsilon = -0.004$ to -0.006: irrigated barley fields.

we have made a validation of the operational method using as reference a digitalized emissivity image constructed with field data, obtaining a good result, which encourages us to continue the study.

We express our gratitude to the Commission of the European Communities (Contracts EPOC-CT90-0030, EV5V-CT91-0033, EV5V-CT91-0035, and TS3-CT-0239) and to the Comisión Interministerial de Ciencia y Tecnología (Contract AMB94-1208) for financial support. We also thank the Ministerio de Educación y Ciencia for the grant received by Mr. Enric Valor. We are indebted to Dr. Y. H. Kerr (LERTS, Toulouse, France) and Dr. J. Zuluaga (INCYTH, Mendoza, Argentina) for providing the Niger AVHRR and the Argentina TM images, respectively, and Dr. B. Lacaze (CEFE / CNRS, Montpellier, France) for supplying the experimental measurements corresponding to the Hérault and the Ardèche areas. Comments and suggestions made by the anonymous referees and by Professor J. A. Sobrino, Dr. C. Coll, Ms. E. Rubio, and Mr. F. Sospedra are also acknowledged.

REFERENCES

Anton, Y. A., and Ross, Y. K. (1990), Emissivity of a soil-vegetation system, *Soviet J. Remote Sens.* 7(5):859–869.

Asrar, G. Ed. (1989), *Theory and Applications of Optical Remote Sensing*, Wiley, New York, pp. 505.

Barth, H. K., and Runge, J. (1993), Land use and vegetation of the pilot area of Barrax, La Mancha, Spain, EFEDA Project Final Report, p. 43.

Becker, F. (1980), In *Remote Sensing Applications in Agriculture and Hydrology* (G. Fraysse, Ed.), Balkema.

Becker, F., and Choudury, B. J. (1988), Relative sensitivity of normalized difference vegetation index (NDVI) and microwave polarization difference index (MPDI) for vegetation and desertification monitoring, *Remote Sens. Environ.* 24: 297–311.

Becker, F., and Li, Z.-L. (1990), Temperature-independent spectral indices in thermal infrared bands, *Remote Sens. Environ.* 32:17–33.

Becker, F., Nerry, F., Ramanantsizehena, P., and Stoll, M. P. (1986), Mesures d'emisivité angulaire par reflexion dans l'infrarouge thermique-implications pour la télédetection, *Int. J. Remote Sens.* 7:1751–1762.

Caselles, V., and Sobrino, J. A. (1989), Determination of frosts in orange groves from NOAA-9 AVHRR data, *Remote Sens. Environ.* 29:135–146.

Caselles, V., Sobrino, J. A., and Coll, C. (1992), A physical model for interpreting the land surface temperature obtained by remote sensors over incomplete canopies, *Remote Sens. Environ.* 39:203–211.

Caselles, V., Coll, C., Valor, E., and Rubio, E. (1995), Mapping land surface emissivity using AVHRR data: Application to La Mancha, Spain, *Remote Sens. Rev.* 12:311–333.

Coll, C. (1994), An operational model to determine the land surface temperature from satellites, Doctoral Thesis, Department of Thermodynamics, University of Valencia [in Spanish].

Coll, C., Caselles, V., and Schmugge, T. J. (1994), Estimation of land surface emissivity differences in the split-window channels of AVHRR, *Remote Sens. Environ.* 48:127–134.

Gillespie, A. R. (1985), Lithologic mapping of silicate rocks using TIMS, in *The TIMS Data Users' Workshop*, JPL Pub. 86-38, pp. 29–44.

Gillespie, A. R., Kahle, A. B., and Walker, R. E. (1986), Color enhancement of highly correlated images. I. Decorrelation and HSI contrast stretches, *Remote Sens. Environ.* 20:209–235.

Coutorbe, J. P. (ed.) (1993), HAPEX-Sahel Report for contract EV5V-CT91-0033 of the Commission of the European Communities, First Report (July 1992–June 1993), CNRM, Toulouse.

Coutorbe, J. P., Lebel, T., Tinga, A., Dolman, H., Engman, E. T., Gash, J. H. C., Kabat, P., Kerr, Y. H., Monteny, B., Prince, S., Sellers, P., Wallace, J. S., Hoepffner, M. (1992), Experimental plan for HAPEX-Sahel, ORSTOM, Montpellier.

Hook, S. J., Gabell, A. R., Green, A. A., and Kealy, P. S. (1992), A comparison of techniques for extracting emissivity information from thermal infrared data for geologic studies, *Remote Sens. Environ.* 42:123–135.

Kahle, A. B., Madura, D. P., and Soha, J. M. (1980), Middle infrared multispectral aircraft scanner data: Analysis for geologic applications, *Appl. Opt.* 19:2279–2290.

Kealy, P. S., and Hook, S. J. (1993), Separating temperature and emissivity in thermal infrared multispectral scanner

data: Implications for recovering land surface temperatures, *IEEE Trans. Geosci. Remote Sens.* 31(6):1155–1164.

Kerr, Y. H., Valero, T., and Wagner, S. (1993), *HAPEX-Sahel Information System CD-ROM 1 & 2 AVHRR 92*, LERTS, CNES, ORSTOM.

Kreith, F. (1962), *Radiation Heat Transfer*, International Textbook Company, Scranton, PA.

Li, Z.-L., and Becker, F. (1990), Properties and comparison of temperature-independent thermal infrared spectral indices with NDVI for HAPEX data, *Remote Sens. Environ.* 43:67–85.

Li, Z.-L., and Becker, F. (1993), Feasibility of land surface temperature and emissivity determination from AVHRR data, *Remote Sens. Environ.* 43:67–85.

Nerry, F., Labed, J., and Stoll, M. P. (1990), Spectral properties of land surfaces in the thermal infrared 2. Field method for spectrally averaged emissivity measurements. *J. Geophys. Res.* 95 (B5):7027–7044.

Olioso, A. (1995), Simulating the relationship between thermal emissivity and the normalized difference vegetation index, *Int. J. Remote Sens.* 16(16):3211–3216.

Owe, M., and van de Griend, A. A. (1994), Ground based measurement of surface temperature and thermal emissivity, *Adv. Space Res.* 14(3):45–48.

Price, J. C. (1990), Using spatial context in satellite data to infer regional scale evapotranspiration, *IEEE Trans. Geosci. Remote Sens.* 28(5):940–948.

Rouse, J. W., Haas, R. H., Schell, J. A., Deering, D. W., and Harlan, J. C. (1974), Monitoring the vernal advancement of retrogradation of natural vegetation, NASA / GSFC, Type III, Final Report, Greenbelt, MD, p. 371.

Rubio, E., Caselles, V., and Badenas, C. (1996), Emissivity measurements of several soils and vegetation types in the 8-14 μm waveband: Analysis of two field methods, *Remote Sens. Environ.*, in press.

Salisbury, J. W., and D'Aria, D. M. (1992), Emissivity of terrestrial materials in the 8-14 μm atmospheric window, *Remote Sens. Environ.* 42:83–106.

Saunders, R. W., and Kriebel, K. T. (1988), An improved method for detecting clear sky and cloudy radiances from AVHRR data, *Int. J. Remote Sens.* 9:123–150.

Schmugge, T. J. (1990), Radiometry at infrared and microwave frequencies, in *ESA / NASA International Workshop*, pp. 1–12.

Soha, J. M., and Schwartz, A. A. (1978), Multispectral histogram normalization contrast enhancement, in *Proceedings, 5th Canadian Symposium on Remote Sensing*, Victoria, British Columbia, Canada, pp. 86–93.

Stoll, M. P., and Pion, J. C. (1993), In *HAPEX-Sahel 1992, Campagne de mesures Supersite Central Est* (B. A. Monteny, Ed.), ORSTOM, Avril 1993.

Sutherland, R. A., and Bartholic, J. F. (1977), Significance of interpreting thermal radiation from a terrestrial surface, *J. Appl. Meteorol.* 16:759–763.

van de Griend, A. A., and Owe, M. (1993), On the relationship between thermal emissivity and the normalized difference vegetation index for natural surfaces, *Int. J. Remote Sens.* 14:1119–1131.

Vidal, A. (ed.) (1994), Proceedings of the Workshop on Thermal Remote Sensing, CEMAGREF Editions, La Londe Les Maures, France, p. 69 [Conclusions and Recommendations on Emissivity].

Watson, K. (1992a), Two-temperature method for measuring emissivity, *Remote Sens. Environ.* 42:117–121.

Watson, K. (1992b), Spectral ratio method for measuring emissivity, *Remote Sens. Environ.* 42:113–116.